Chronic Exposure of Adult Rats to Low Doses of Methylmercury Induced a State of Metabolic Deficit in the Somatosensory Cortex

ARTICLE *in* JOURNAL OF PROTEOME RESEARCH · AUGUST 2013

Impact Factor: 4.25 · DOI: 10.1021/pr400356v · Source: PubMed

4 AUTHORS, INCLUDING:

Ming Hung Wong
The Hong Kong Institute of Education
812 PUBLICATIONS **22,073** CITATIONS
SEE PROFILE

Laurie Hing Man Chan
University of Ottawa
203 PUBLICATIONS **4,810** CITATIONS
SEE PROFILE

Journal of proteome research

Article

pubs.acs.org/jpr

Chronic Exposure of Adult Rats to Low Doses of Methylmercury Induced a State of Metabolic Deficit in the Somatosensory Cortex

Hang-Kin Kong,[†] Ming-Hung Wong,[‡] Hing-Man Chan,[†,§] and Samuel Chun-Lap Lo*[,†]

[†]Food Safety and Technology Research Centre, The Department of Applied Biology and Chemical Technology, The Hong Kong Polytechnic University, Room Y810, Lee Shau Kee Building (Block Y), Hung Hom, Hong Kong, China

[‡]The Croucher Foundation of Environmental Sciences, Hong Kong Baptist University, 224 Waterloo Road, Kowloon Tong, Hong Kong, China

[§]Centre for Advanced Research in Environmental Genomics, University of Ottawa, 20 Marie-Curie, Ottawa K1N 6N5, Canada

Supporting Information

ABSTRACT: Because of the ever-increasing bioaccumulation of methylmercury (MeHg) in the marine food chain, human consumers are exposed to low doses of MeHg continually through seafood consumption. Epidemiological studies strongly suggest that chronic prenatal exposure to nanomolar of MeHg has immense negative impacts on neurological development in neonates. However, effects of chronic exposure to low doses (CELDs) of MeHg in adult brains on a molecular level are unknown. The current study aims to investigate the molecular effects of CELD of MeHg on adult somatosensory cortex in a rat model using proteomic techniques. Young adult rats were fed with a low dose of MeHg (40 μg/kg body weight/day) for a maximum of 12 weeks. Whole proteome expression of the somatosensory cortex (S1 area) of normal rats and those with CELD to MeHg were compared. Levels of MeHg, total calcium, adenosine triphosphate (ATP), and pyruvate were also measured. Comparative proteomic studies of the somatosensory cortexes revealed that 94 proteins involved in the various metabolic processes (including carbohydrate metabolism, generation of precursors for essential metabolites, energy, proteins, cellular components for morphogenesis, and neurotransmission) were down-regulated. Consequently, levels of important end products of active metabolism including ATP, pyruvate, and total calcium were also found to be significantly reduced concomitantly. Our results showed that CELD of MeHg induced a state of metabolic deficit in the somatosensory cortex of adult rats.

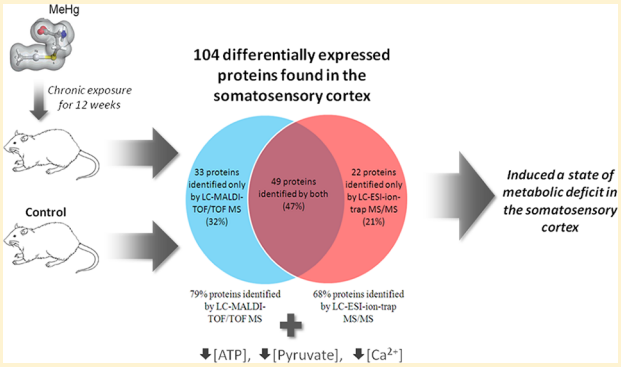

KEYWORDS: *methylmercury, somatosensory cortex, chronic exposure, proteomic*

INTRODUCTION

Methylmercury (MeHg) is an environmental contaminant found in seafood that bioaccumulates and biomagnifies along the marine food chain.[1] It is said that through fish consumption humans are chronically exposed to MeHg. According to the World Health Organization, there are one billion people who rely on fish as their main source of food intake. Hence, these people are exposed to MeHg continually.

A recent cohort study on Hong Kong children revealed that prenatal exposure to low doses of MeHg resulted in long-term neurocognitive impacts.[2] Other cohort studies had reported various negative impacts of chronic exposure to low dose (CELD) of MeHg on children, including abnormal vision condition,[3] auditory deficits,[4] and neurobehavioral deficits.[5] Adverse effects of methylmercury on developing neonates are well-documented and reviewed.[6,7] Some of the adverse effects included decreased motor functions, attention deficit, decreased visuospatial performance, decreased neurologic optimality score, decreased coordination of the legs, and so on.[6,7] However, the effects of CELD of MeHg on adults are unclear. The provisional tolerable weekly intake (PTWI) of 1.6 μg MeHg/kg body weight was recommended by the Joint FAO/WHO Expert Committee on Food Additives (JECFA) in 2003 and remains unchanged. JECFA considered that taking up to two times the PTWI would not pose an increased risk of neurotoxicity in adults, except for pregnant women for protection of the fetus. However, a seafood consumption survey conducted in 2009 in Murcia, Spain found that ∼54% of children, 10% of pregnant women, and 15% of women of childbearing age had a MeHg intake that exceeded the PTWI limit of MeHg.[8] In 2008 in Hong Kong, The Centre of Food Safety of the Government estimated that 5% of the secondary school students in Hong Kong had an average dietary exposures to MeHg of ∼1.61 μg/kg bw (body weight)/week, that is, 94−106% of PTWI.[9] Furthermore, measurements of Hg

Special Issue: Agricultural and Environmental Proteomics

Received: April 17, 2013
Published: August 15, 2013

   dx.doi.org/10.1021/pr400356v | J. Proteome Res. 2013, 12, 5233−5245

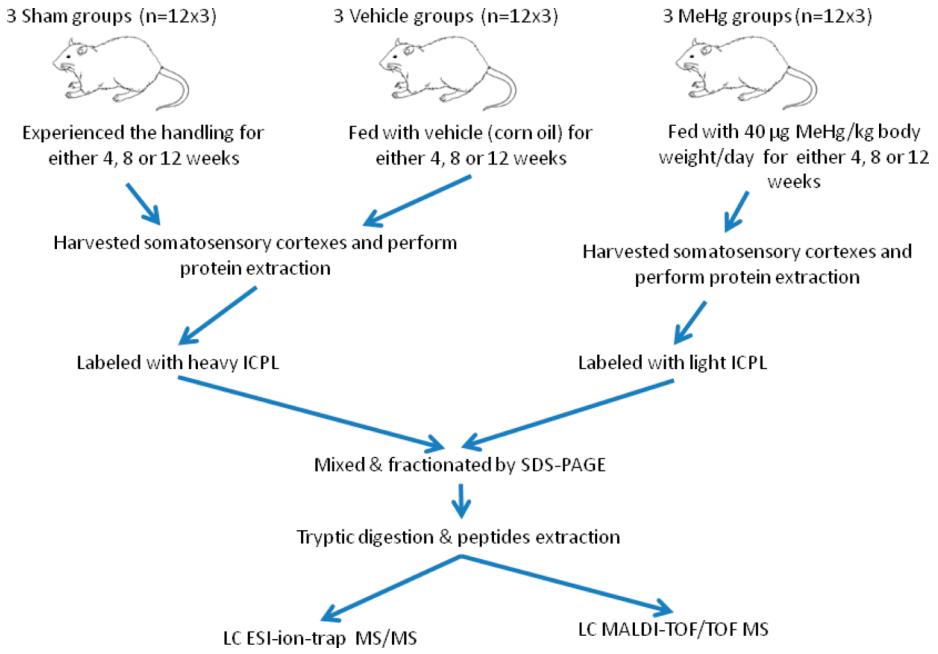

Figure 1. Treatment schedule of the three groups of rats.

content in hair samples collected from fish-dependent populations around the world, including Canada,[10] Faroe Islands,[11] Greenland,[12] China,[13] New Zealand,[14] and the Seychelles islands,[15] showed that the values were higher than those of other populations, ranging from 40 to 10 ppm. Normal values of apparently uncontaminated individuals were about 0.1−12 ppm.[16] Hence, through seafood consumption in fish-dependent populations, these data indicated that it is common for people to have MeHg intake that exceeds the PWTI. It is speculated that the MeHg accumulated in the human body would eventually induce negative effects on health. In 2008, a longitudinal study conducted on the Faroe Islands showed that lifelong exposure to MeHg is positively associated with Parkinson's disease (PD).[17] However, fish serve as a major source of protein intake, and the polyunsaturated fatty acids (PUFAs) present in fish meat are very important for supporting a healthy circulatory system as well as providing essential building blocks for brain development in neonates. Because consumption of fish is of important nutrition value, there is a strong need to understand the effects of CELD of MeHg so that subsequent risk-benefit estimations of fish consumption can be performed.[18]

It is known that one of the early signs of acute Hg overdose in human is paresthesia. In the historic incidence of acute large dose poisoning of Hg in Minamata, it was found that when the hair Hg levels in patients reached 50 ppm, they began to suffer from sensory loss.[19,20] In 2004, Miyaoka and coworkers conducted psychophysical sensory examination on people with a history of MeHg exposure and found that they had sensory disturbances. This abnormality is due, predominately, to damages in the somatosensory area (S1 area) in the cerebral cortex.[21] Therefore, the somatosensory cortex could be one of the primarily affected sites by the MeHg accumulated.

In the past few decades, many studies have been conducted to understand the mechanism underlying MeHg toxicology. Most of these studies were performed using cell culture models. Usually micromolar or higher levels of MeHg were used. With cell cultures, for example, increased intracellular calcium ion levels,[22] increased production of reactive oxygen species (ROS),[23] mitochondrial dysfunction,[24] and inhibition of tubulin polymerization[25] were observed when neuronal cells, neuroblastoma cells, or astrocytes were exposed to micromolar levels of MeHg. Numerous experiments using laboratory animals have confirmed the toxic effects of MeHg on reproduction and offspring neurobehavioral function. Most of these animal studies have examined the sensitivity of the developing rodent fetus to maternal MeHg exposure.[26−30] Developmental anatomical indices and auditory startle measurements have been suggested[27,29,30] to be appropriate end points for the evaluation of MeHg-induced toxicity. However, studies on effects in adults often use a much higher dose at milligram levels of MeHg. For example, ICR mice administered with daily injections of 1 or 3 mg MeHg/kg body weight from postnatal days 15 to 17 showed reduced memory and spatial orientation.[31] B6C3F1/HSD mice administrated with 1 and 3 ppm lifelong showed delayed spatial alternation.[32] Working memory was impaired in female C57BL/6 mice administrated with 6 or 8 ppm of MeHg for 6 weeks or more.[33] In rats administrated with 400 μg MeHg/kg body weight/day, symptoms including delayed hind limb crossing, gait disorders, and diminished running wheel activity were observed.[34] However, no observable abnormality was observed in rats taking 40 μg MeHg/kg body weight/day in the same study.[34] In monkeys, despite observation of some abnormal morphological changes in the microglial cells, intake of 50 μg of MeHg/kg body weight daily for up to 18 months did not cause any observable neurological deficiency.[35] Taken overall, these previous studies usually used high levels of MeHg in their studies, and most studies did not investigate the effects of MeHg administration in vivo at the molecular level. After the two large-scale incidences of acute MeHg intoxication (in Minamata in the 1950s as well as in Iraq in 1971), most countries are very conscious about safety levels of MeHg in food. Hence, acute overdose of MeHg exposure is considered to be unlikely. However, as previously stated, the effects of chronic exposure to sub-milli-molar or even sub-micro-molar range of MeHg may not induce visible symptoms, and their molecular effects are unknown. Furthermore, because consuming fish has numerous

health benefits including a reduced risk of cardiovascular disease and many people consume fish as their major food intake, it is important to find the effects of CELD of MeHg. Therefore, as a first step to understand the molecular effects of CELD intake of MeHg in the brain, we conducted a comparative proteomic study on S1 areas from control rats and rats with CELD intake of MeHg.

MATERIALS AND METHODS

MeHg Intoxication and Harvesting of Somatosensory Cortexes

Six- to eight-week-old Sprague−Dawley (SD) rats (200 to 220 g) used in this study were provided by Specific-Pathogen-Free Animal Facilities of the Shenzhen Research Institute of the Hong Kong Polytechnic University (HKPU). The rats were housed at a constant temperature of 21 to 22 °C and a 12 h light/dark cycle in accordance with the recommendation of the Animal Subjects Ethics Subcommittee (ASESC) of the HKPU. Food and water were provided ad libitum. All procedures performed on the rats were approved by the ASESC of the HKPU.

At every time point (4, 8, and 12 weeks), the rats were randomly divided into the sham control, vehicle, and MeHg groups. Each group contained 12 animals. Rats in the MeHg group were fed by oral gavage with 40 μg of MeHg in corn oil/kg of body weight/day. In a previous study reported by Day and coworkers, rats fed with 40 μg of MeHg/kg body weight/day for ∼18 months did not show any common high-dose MeHg intoxication symptoms such as hind limb crossing, gait disorders, and diminished running wheel activities.[34] This dosage that does not cause visible neurological effect was chosen to maximize effects of CELDs of MeHg. Further work could be performed to address effects at lower levels. The whole feeding experiment of each subgroup of vehicle/MeHg treatment was performed for 4, 8, or 12 weeks. Administrated doses of MeHg were adjusted every 2 weeks according to the increase in the body weight of the rats. Corn oil (Southseas Oils & Fats Industrial (Chi Wan) Limited, Hong Kong), was used to feed the rats in the vehicle group by oral gavage (0.1 mL of corn oil/day). Rats in the sham group received the feeding procedures but without either MeHg or the vehicle. Figure 1 summarized the feeding schedule of the experiments. At the end of designated feeding period, rats in the experiment were sacrificed for their brains. Blood vessels on the brains were removed and the brains were washed immediately with cold phosphate-buffered saline (PBS) pH 7.4. Subsequently, somatosensory cortexes were harvested based on known "landmarks" from the rat brain stereotaxic atlas. The tissues collected were stored at −80 °C before use and no sample was stored for more than 6 months.

Quantification of tHg and Ca by Inductively Coupled Plasma Mass Spectrometer

Somatosensory cortex samples were processed according to procedures reported by Rodrigues et al. with modifications.[36] Ultra pure water was used in the quantification process. In brief, ∼0.1 g brain tissue was mixed with 2.9 mL of concentrated (60%) HNO_3 (Merck, USA) and 0.1% (v/v) 2-mercaptoethanol in a 15 mL polypropylene tube before being sonicated for 15 min twice. Subsequently, the samples were diluted with 1% (v/v) HNO_3 that contained 500 ppb of gold ($AuCl_4$) (Merck, USA). The samples were then filtered with 0.2 μm nylon filters prior to analysis by an inductively coupled plasma mass spectrometer (ICP-MS) (7500cx from Agilent Technology, USA). Five ppb of indium ($In(NO_3)_3$) (Merck, USA) was added to each sample to serve as an internal standard for ICP-MS measurements. Counts per second (cps) of ^{44}Ca, ^{113}In, and ^{202}Hg were measured. All samples were measured in triplicate. Amounts of total mercury (tHg) and Ca in somatosensory cortexes harvested from different groups and at different time points were compared by one-way (ANOVA) and posthoc Bonferroni test.

Protein Extraction and Isotope-Coded Protein Labeling

Comparative proteomics using isotope-coded protein labeling (ICPL) labeling techniques was performed as previously described with modifications.[37] In brief, 0.1 g somatosensory cortex was homogenized in 100 μL of lysis buffer provided in the ICPL kit (Bruker, Germany). The sample was centrifuged at 13 000*g* at 4 °C for 15 min. Protein concentrations of the supernatants collected were determined by the Bradford assay. Six samples each from the vehicle and MeHg groups (fed for 12 weeks and $n = 6$ for each group) were used in proteomic comparisons. Extracts from each part of the brains of rats in the same group were mixed equally and analyzed in triplicate. As for the labeling procedure, it was performed according to recommendations from the manufacturer. In brief, 100 μg of protein from each of the vehicle and MeHg groups (each in 20 μL) was used. Each sample was allowed to react at 55 °C for 1 h with 0.5 μL of the reducing agent provided in the ICPL kit. Subsequently, the samples were alkylated in the dark and at room temperature for 30 min with 0.5 μL of IAA reagent provided in the kit. Samples of the vehicle group were labeled with heavy ICPL, while those of the MeHg group were labeled with light ICPL under the same conditions. Subsequently, 2 μL of stop solution was added to both samples to stop the labeling process. The two samples for comparison present in identical volumes and protein amounts were mixed before being precipitated with acetone overnight at −20 °C. After overnight precipitation, the proteins were dissolved in 10 μL of lysis buffer (7 M urea, 2 M thiourea, 4% CHAPS, 40 mM Tris, pH 8.6) before sodium dodecyl sulfate polyacrylamide gel electrophoresis (SDS-PAGE).

Sodium Dodecyl Sulfate Polyacrylamide Gel Electrophoresis

Ten μL of 2× gel loading buffer (0.25 M Tris HCl, pH 6.8, 10% (w/v) SDS, 50% (v/v) glycerol, 1% (v/v) β-mercaptoethanol, 0.01% (v/v) bromophenol blue) was added to the labeled mixture, then heated until boiling for 5 min in a water bath. The mixture was resolved on a 10% acrylamide gel. After electrophoresis, the SDS-PAGE gel was visualized using Coomassive stain (0.1% Coomassive Blue R 250 in 10% acetic acid and 40% methanol). The gel lane containing the mixture was cut into 2 mm thick gel slides for further analysis.

Proteases Digestion

Each gel slide was reduced with 10 mM DTT and alkylated with 55 mM IAA. Enzymatic digestion was performed overnight using sequencing-grade modified trypsin (Promega, USA) and endoproteinase GluC (Sigma Aldrich, USA) at 37 °C. The digested peptides were extracted with 50% (v/v) acetonitrile (ACN) and 1% (v/v) trifluoroacetic acid. Ultrasonication was applied to facilitate diffusion of peptides out of the gel slide. Subsequently, the extracted peptides were dried under vacuum and 10 μL of 2% ACN and 0.1% formic acid (FA) were added to resuspend the extracted peptides.

Nano C18 Liquid Chromatography and Fractionation By PROTEINEER fc II

A nanoflow C18 column, 15 cm in length and 75 μm in inner diameter (LC PACKINGS, Netherlands) was used to separate

dx.doi.org/10.1021/pr400356v | J. Proteome Res. 2013, 12, 5233−5245

the extracted peptides. Optimization of the flow rates as well as operation of the nano-LC chromatographic system was performed according the protocol recommended by Bruker, Germany. The column was first equilibrated in 0.1% FA before being loaded with 1 μg of peptides mixture from each gel slide. Temperature of the column was kept at 40 °C by a column heater. Peptides in the column were eluted with a linear gradient containing 20% ultra pure water, 80% ACN, and 0.001% TFA in a linear gradient of 4−80% and at a flow rate of 450 nL/min for ∼120 min. The column was chased with 100% elution buffer (20% ultra pure water, 80% ACN, and 0.001% TFA) for another 10 min. Peptides eluted from the column were divided into two equal parts with an in-house homemade splitter. Half of the peptides were applied online directly into an ESI-ion-trap MS/MS mass spectrometer (HCT ultra from Bruker, Germany). The other half of the peptides were spotted automatically onto a 800−384 anchor chip (Bruker, Germany) with a matrix solution (saturated α-cyano-4-hydroxycinnamic acid (HCCA) in 60% ethanol, 30% acetone, and 10% 0.1% TFA) by an LC-MALDI fraction collector (PROTEINEER fc II from Bruker, Germany). Each sample spot represented eluate collected over 15 s of elution from the splitter. After fractionation, samples on the anchor chip were analyzed by a MALDI-TOF/TOF MS (Autoflex III from Bruker, Germany) in the positive mode.

ESI-Ion-Trap MS/MS Spectrometry and Data Analysis

The ESI-ion-trap MS/MS spectrometer was operated in the data-dependent acquisition mode. Positive ions within the m/z range of 400 to 1800 and signal/noise (S/N) ratios higher than 4 were selected for MS/MS fragmentation analysis. Accumulation time for a survey scan was set at 100 ms. Subsequently, five precursor ions with intensities above the threshold values of 10 000 (arbitrary unit of strength of signals) were analyzed. Individual precursor ions that appeared in two successive injections were excluded for analysis for 1 min. Relative collision energy was set to be 1 V. MS/MS data collected from the ESI-ion-trap MS/MS spectrometric analysis were searched against the National Center for Biotechnology Information non-redundant (NCBInr) database (release 50 dated Nov 8, 2011) using WrapLC 1.2 and Biotool 3.1 (Bruker, Germany) coupled to Mascot v2.2. The taxonomy was set at "*Rattus*" (139 968 sequences). In the search, the modifications selected were "ICPL labeled at lysine and N-terminal of the protein", "oxidation of methionine", and "carbamidomethylation of cysteine". The mass tolerance of MS was set at 0.6 Da, and the mass tolerance of MS/MS was set at 1.2 Da. The charge states were set to be 2+ and 3+. Cleavage sites of the proteases were set to "C-terminal of arginine and glutamate". The significance threshold of ion score was set at 0.05. Peptides with the ion scores higher than the threshold were considered to be positively identified. Target-decoy strategy was employed to determine false discovery rate (FDR) as described by Bruker, manufacturer of the ESI-ion-trap MS/MS spectrometer. A random sequence database was used as the decoy database. FDR was defined as the number of validated decoy hits/(number of validated target hits + number of decoy hits)*100 using the Mascot algorithm. FDR of the protein identifications of the ICPL data was <1%.

MALDI-TOF/TOF MS and Data Analysis

MALDI-TOF/TOF MS analysis of the peptides spotted onto the anchor chip was performed with a Bruker Autoflex III (Germany). Amino-acid sequence tags were generated with the Autoflex III operated in the positive reflectron mode. External calibration was performed using Bruker peptide mix calibration standard, and internal calibration was carried out using enzyme autolysis peaks. For precursor ion scanning, ions with the m/z ratios 700 to 3500 were selected. The laser power was set at 30%. Spectra of 500 shots were accumulated for each sample spot on the anchor chip. Running in an automatic mode, the laser moved randomly to another position of the same spot after every 50 laser shots. For MS/MS fragmentation, same as the ESI-ion-trap MS/MS, precursor ions with S/N ratio higher than 4 were selected. The laser power was set at 45%. Also, in an automatic manner, spectra of 1500 shots were accumulated for one sample spot, and the laser moved randomly to another position of the same spot after every 100 shots. The MS/MS data were searched against the NCBInr database (release 50 dated Nov 8, 2011) using WrapLC 1.2 and Biotool 3.1 coupled to Mascot v2.2. The taxonomy was set at "*Rattus*" (139968 sequences). The modifications selected were "ICPL labeled at lysine and N-terminal of the protein", "oxidation of methionine", and "carbamidomethylation of cysteine". Cleavage sites of the proteases were set to "C-terminal of arginine and glutamate". Further in the bioinformatic search, mass tolerance of the peak mass accuracy was set at 50 ppm, and that of the mass tolerance of MS/MS was set at 0.6 Da. The charge state was set at 1+. The significance threshold of ion score was set at 0.05. Peptides with ion scores higher than the threshold were considered as positively identified. Same as that described in the ESI-ion-trap MS/MS operation, target-decoy strategy with a randomly generated decoy database was employed to determine FDR. FDR was defined as the number of validated decoy hits/(number of validated target hits + number of decoy hits)*100 using the Mascot algorithm. FDR of protein identifications of the ICPL data in the MALDI-TOF MS operation was found to be <1%.

Identification of Differentially Expressed Proteins

Before computation on whether there was significant variation of expression for each of the protein identified, minimum technical variability of the current system was calculated according to methodologies suggested by the manufacturer of the ICPL kit (Bruker, Germany). In brief, a protein mixture used previously for the LC-gradient elution optimization was divided into two identical portions with the same protein amount in the same volume. One portion was labeled with light ICPL, and the other one was labeled with heavy ICPL. Subsequently, the two labeled samples were mixed together (1:1) before proteomic analysis. Relative intensities of most of the ICPL pairs were almost the same, which indicated a high level of reproducibility and accuracy of the labeling. Relative intensities of 100 ICPL pairs were used to calculate the experimental value of the quantification of the relative abundance of labeled peptides in the 1:1 mixed sample. As shown in Table S1 in the Supporting Information, mean technical variabilities of LC-ES-ion-trap MS/MS and LC-MALDI-TOF/TOF MS ± 2 standard deviations (2 S.D.) were found to be 0.96 ± 0.16 and 0.86 ± 0.11, respectively. Both of the experimental quantifications were close to 1, and the relative abundance of peptides in the mixture was found to be normally distributed (data not shown). The determination was performed in triplicate, and the results obtained were comparable to those previously described.[38,39] Subsequently, MS spectral data obtained from the MALDI-TOF/TOF as well as ESI-ion-trap MS, including amino acid sequences tags, peptide mass fingerprints, and mass spectra for each of the gel slice, were combined using WrapLC 1.2 to generate a full list of proteins identified and their relative expression levels calculated between the vehicle and MeHg groups. Relative quantification of the

Table 1. Primary Antibodies Chosen for Validation Experiments with Western Blot

names of protein	catalog code[a]	host	reactivity[b]	clonality	dilution used in Western blot
enolase 2, gamma, neuronal	NB100-91898	rabbit	H, M, R	polyclonal	1:1000
ATP synthase beta subunit	NB600-1171	mouse	H, M, R	monoclonal	1:1000
eukaryotic translation elongation factor 2	NB100-79935	rabbit	H, M, R	monoclonal	1:2000
synapsin I isoform a	NBP1-19903	rabbit	H, M, R	polyclonal	1:1000
vesicle associated membrane protein 2B	NB100-91352	rabbit	H, M, R	polyclonal	1:3000
dynamin 1	NB110-56934	rabbit	H, M, R	monoclonal	1:2000
neuron-specific class III beta-tubulin	NB600-1018	mouse	all mammals	monoclonal	1:10000
platelet-activating factor acetylhydrolase IB subunit alpha	NBP1-03125	rabbit	H, M, R	polyclonal	1:1000
microtubule-associated protein 2, isoform CRA_b	NB600-1372	mouse	H, M, R	monoclonal	1:500
Na+/K+ -ATPase alpha 2 subunit precursor	NBP1-00937	rabbit	H, M, R	polyclonal	1:1000

[a]All of the antibodies used were purchased from Novus Biologicals, USA. [b]H: human, M: mouse, R: rat.

expression level of a protein in the somatosensory cortex was determined by the ratio of peak areas of peptides assigned to that protein labeled with either heavy or light ICPL. The ratio was reported as the percentage change in the peak area. The significant threshold for differentially expressed proteins was fixed at the two standard deviation values from the mean of the ratio calculated from previous experiment that computed the technical variabilities (see previous and Supporting Information Table S1). On the basis of the experimental data obtained, a protein with either a differential decrease/increase of 32% in expression in the ESI-ion-trap MS/MS system or a differential decrease/increase of 22% in expression in the MALDI-TOF/TOF system was taken as significantly differentially expressed.

Pathway Analysis Using Gene Orthology

Protein analysis through evolutionary relationships classification system (PANTHER) classifies genes by their functions and predicts their functions using known experimental evidence and evolutionary relationships. The system is available freely online (http://www.pantherdb.org/) and was used to analyze the proteomic data obtained. It was intended to pinpoint pathways that may be collectively affected by bioaccumulation of MeHg in the somatosensory cortex. The list of the differentially expressed proteins was uploaded into the PANTHER Batch ID Search "http://www.pantherdb.org/genes/batchIdSearch.jsp" against the "Rattus norvegicus" database. The differentially expressed proteins were clustered into different gene ontology (GO) terms, including biological process, molecular functions, cellular component, protein functions, and pathways automatically. The proteomic data were also analyzed using the Kyoto Encyclopedia of Genes and Genomes (KEGG, http://www.genome.jp/kegg) and Protein Knowledgebase (UniProtKB in UniProt, http://www.uniprot.org/) as cross-references. The results generated from the analysis were presented in a pie chart automatically, showing the percentage of the differentially expressed proteins that are known to be involved in the same biological process.

Western Blotting

Western blotting (WB) was employed to validate some of the results obtained from ICPL analysis. Ten μg of protein samples extracted from the somatosensory cortexes (n = 5 in each group) was resolved by 10% SDS-PAGE and subsequently transferred onto a 0.45 μm nitrocellulose membrane (Millipore, USA) using previously described methodologies.[40] Details of the primary antibodies used in these verification experiments are shown in Table 1. After incubation with the first antibodies and subsequent washing steps, the membranes were incubated with corresponding secondary antibodies that were linked with horseradish peroxidase (HRP). Finally, after washing, the Western blots were visualized with HRP substrate (Supersignal West Pico Chemiluminescence Kit, Pierce, USA). The bioluminescence units (BLUs) of the positive protein bands were quantified by the ChemiDoc XRS+ system (Bio-Rad, USA). Expression of each target protein was normalized against expression level of histone 3 (H3) in the same sample. Antihistone H3 antibodies were purchased from Novus Biologicals, USA.

Protein−Protein Interactions Analysis

STRING v9.0, an online freely accessible database (http://string-db.org/) was also used to compute protein−protein interaction (PPI) networks of the differentially expressed proteins found. After loading names of proteins into the database, depth of the network was set at 1 and the species selected for analysis was "Rattus".

Extraction of Adenosine Triphosphate and Pyruvate from the Brain Tissues

Extraction procedures for these metabolites were adopted from protocols published by Khan et al. with modifications.[41] In brief, 200 μL of 10% (v/v) of perchloric acid ($HClO_4$) was added to 0.1 g of brain tissue before homogenizing for 10 s. The homogenized sample was centrifuged at 4000g for 10 min at 4 °C. The collected supernatant was neutralized by the addition of 50 μL of 4 M potassium carbonate (K_2CO_3). After vortexing, the sample was centrifuged at 4000g again for 5 min at 4 °C to remove the precipitated $KClO_4$. The pH of each sample was within 5 to 7. Finally, the sample was diluted with 1× reaction buffer from either the adenosine triphosphate (ATP) determination kit or the pyruvate assay kit for quantification of ATP and pyruvate, respectively.

ATP Assay

An ATP determination kit (Invitrogen, USA) was used, and the procedures were performed as recommended by the manufacturer. Ten μL of blank, standards, or samples was added to the wells of a blank, ice-chilled 96-well microtiter plate. The supernatant prepared after removal of $KClO_4$ from a mixture of 200 μL of 10% of $HClO_4$ and 50 μL of 4 M K_2CO_3 was used as blank. The assay buffer was prepared by mixing 8.9 mL of distilled H_2O, 0.5 mL of 20× reaction buffer, 0.1 mL of 0.1 M DTT, 0.5 mL of 10 mM D-luciferin, and 2.5 μL of 5 mg/mL firefly luciferase together. Ninety μL of the assay buffer was added to each well. After the assay buffer was added, the plate was kept in the dark and the reactants were allowed to react for 15 min. Bioluminescence signals emitted were measured at 560 nm. All blanks, standards, and samples were measured in triplicate. Averaged ATP readings were reported. The amounts of ATP in different parts of the brain of the different groups at each time

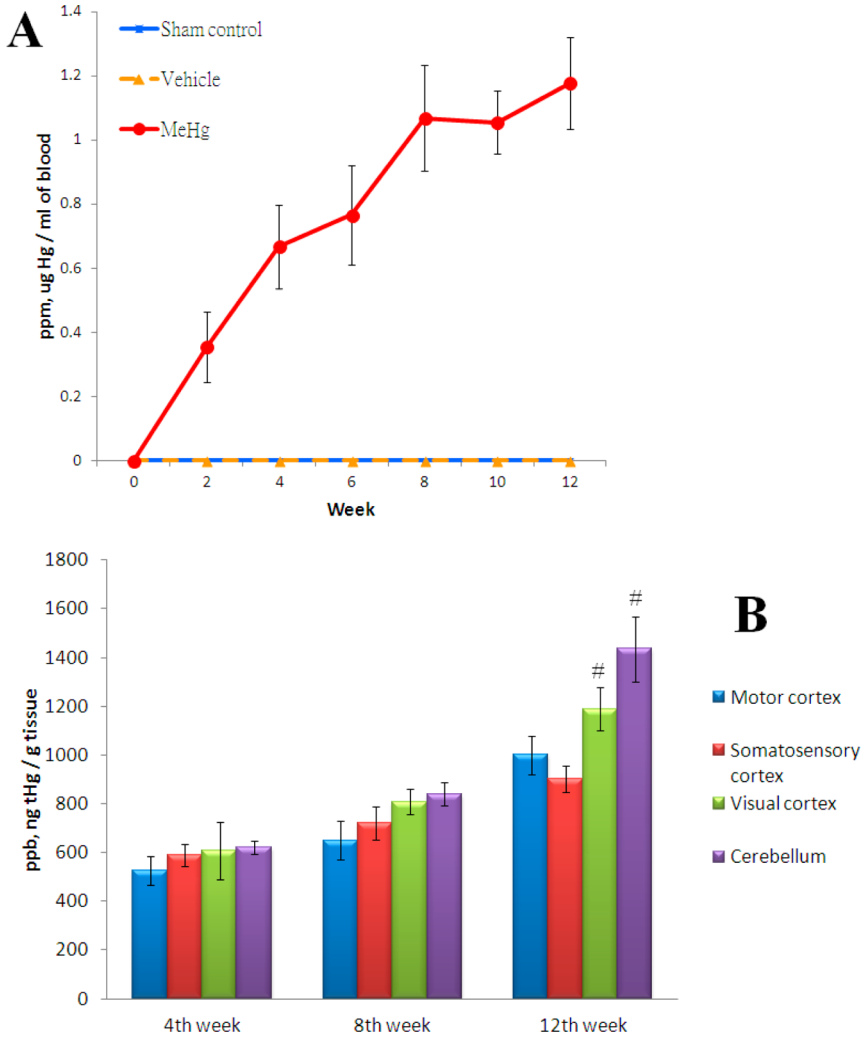

Figure 2. Amount of total mercury (tHg) in the blood samples and different parts of the brains from rats with chronic low-dose administration of MeHg. Each group at each time point contained 12 animals. (A) tHg level in blood. The amount of tHg in the MeHg group gradually increased and reached around 3 to 3.5 ppm after 12 weeks, while only trace amount of tHg could be found in blood samples from the sham control and vehicle groups. (B) tHg level in different parts of the brains harvested in the MeHg group. Overall, longer exposure time resulted in more tHg accumulated in the brains. At the 12th week, the amounts of tHg in the visual cortex and cerebellum were significantly higher than those in the motor and somatosensory cortexes (#, $p < 0.05$).

point were compared by one-way (ANOVA) and posthoc Bonferroni test.

Pyruvate Assay

A pyruvate assay kit was used (Cayman Chemical, USA), and the procedures used were performed according to those recommended by the manufacturer. In brief, 20 μL of blank, standards, or samples was added to wells of a blank ice-chilled 96-well microtiter plate. The supernatant, prepared after mixing 200 μL of 10% $HClO_4$ with 50 μL of 4 M K_2CO_3, was used as blank. The reaction buffer was prepared by mixing 5 mL of 1× assay buffer, a 5 mL mixture of cofactors, 1 mL of fluorometric detector, and 2 mL of enzyme mixture. 130 μL of the reaction buffer was added to each well. After the reaction buffer was added, reactants were allowed to react in the dark for 20 min. The excitation wavelength was set at 535 nm, and the emission wavelength was set at 595 nm. Each sample was measured in duplicate. Amounts of pyruvate in different parts of the brain at each time point and among groups were compared by one-way (ANOVA) and posthoc Bonferroni test.

RESULTS

Quantifications of tHg in Blood and MeHg in Brain

Total mercury (tHg) levels in the serum samples from the three groups of rats are shown in Figure 2A. Total Hg levels of the various parts of the brains harvested from the MeHg group are shown in Figure 2B. (tHg levels of the sham control and vehicle groups are reported in the Supporting Information Table S2.) The increase in body weights of rats in the MeHg group was the same as that in the sham control and vehicle groups (data not shown). No abnormal behavior could be seen in all of the rats used in the experiments. In general, the amounts of tHg found in blood and in various parts of the brain were directly proportional to the duration of exposure to MeHg. Our data showed that MeHg fed orally was absorbed into the body and accumulated in various parts of the brain.

CELD of MeHg Down-Regulated Proteins Involved in Various Metabolic Pathways in S1 Area

Because the somatosensory cortexes seem to be one of the first sites affected by acute mercury intoxication, the whole proteome

dx.doi.org/10.1021/pr400356v | J. Proteome Res. 2013, 12, 5233−5245

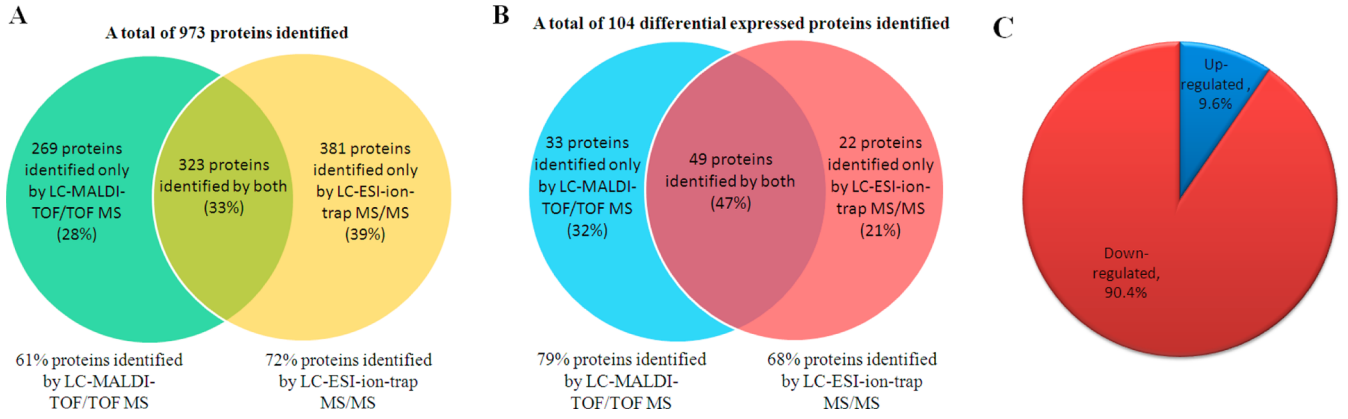

Figure 3. Proteins that were found to be differentially expressed in somatosensory cortexes from rats fed with MeHg. (A) 333 proteins were identified by both techniques: 269 and 381 proteins were uniquely identified by LC-MALDI-TOF/TOF MS and LC-ESI-ion-trap MS/MS, respectively. (B) 49 differentially expressed proteins identified by both techniques. 33 and 22 differentially expressed proteins were identified uniquely by LC-MALDI-TOF/TOF MS and LC-ESI-ion-trap MS/MS, respectively. (C) Nearly 90% of the differentially expressed proteins were down-regulated while the remaining 10% were up-regulated.

Table 2. Comparison of the Results Obtained with the Three Methods for Quantification of Protein Expression Levels

		change in expression as quantified by					
		LC-ESI-ion trap MS/MS[a]		LC-MALDI-TOF/TOF MS[a]		Western blotting[b]	
protein name	NCBInr accession no.	fold change[c]	% change[d]	fold change[c]	% change[d]	fold change[c]	% change[d]
Enolase 2, gamma, neuronal [*Rattus norvegicus*]	gil26023949	↓ 0.55 ± 0.21	↓ 45 ± 21	↓ 0.59 ± 0.15	↓ 41 ± 15	↓ 0.52 ± 0.06	↓ 48 ± 6
ATP synthase beta subunit [*Rattus norvegicus*]	gil1374715	↓ 0.62 ± 0.05	↓ 38 ± 5	↓ 0.43 ± 0.09	↓ 57 ± 9	↓ 0.46 ± 0.03	↓ 54 ± 3
eukaryotic translation elongation factor 2 [*Rattus norvegicus*]	gil8393296	↓ 0.63 ± 0.08	↓ 37 ± 8	↓ 0.48 ± 0.04	↓ 52 ± 4	↓ 0.50 ± 0.07	↓ 50 ± 7
synapsin I isoform a [*Rattus norvegicus*]	gil9507159	[e]	[e]	↓ 0.58 ± 0.03	↓ 42 ± 3	↓ 0.46 ± 0.08	↓ 54 ± 8
vesicle-associated membrane protein 2B [*Rattus norvegicus*]	gil4894188	↑ 3.26 ± 0.55	↑ 226 ± 55	↑ 4.73 ± 0.80	↑ 373 ± 80	↑ 2.14 ± 0.31	↑ 114 ± 31
dynamin 1 [*Rattus norvegicus*]	gil18093102	↓ 0.60 ± 0.02	↓ 40 ± 2	↓ 0.52 ± 0.03	↓ 48 ± 3	↓ 0.49 ± 0.05	↓ 51 ± 5
neuron-specific class III beta-tubulin [*Rattus norvegicus*]	gil20799322	[e]	[e]	↓ 0.44 ± 0.05	↓ 56 ± 5	↓ 0.79 ± 0.10	↓ 21 ± 10
platelet-activating factor acetylhydrolase IB subunit alpha [*Rattus norvegicus*]	gil13929078	↓ 0.53 ± 0.07	↓ 47 ± 7	↓ 0.42 ± 0.06	↓ 58 ± 6	↓ 0.50 ± 0.05	↓ 50 ± 5
microtubule-associated protein 2, isoform CRA_b [*Rattus norvegicus*]	gil 149016020	↓ 0.58 ± 0.14	↓ 42 ± 14	[e]	[e]	↓ 0.62 ± 0.10	↓ 38 ± 10
Na+/K+ -ATPase alpha 2 subunit precursor [*Rattus norvegicus*]	gil6978545	[e]	[e]	↑ 1.75 ± 0.15	↑ 75 ± 15	↑ 1.49 ± 0.12	↑ 49 ± 12

[a]For the LC-ESI-ion-trap MS/MS and LC-MALDI-TOF/TOF MS, six animals from each of the vehicle and MeHg treatment groups were used. [b]For the Western blotting validation experiment, five animals from each of the vehicle and MeHg treatment groups were used. [c]Fold change was expressed as mean fold change followed by standard deviation. Fold change was calculated by dividing mean of the total peak areas of peptides of the designated protein expressed in the MeHg group by mean of the peak areas of peptides of corresponding protein expressed in the vehicle group. ↑ means increase, while ↓ means decrease. [d]Percentage change in expression was expressed as mean % change followed by standard deviation. % change was calculated by the formula = (mean of the total peak areas of peptides of the designated protein expressed in the MeHg group − mean of the peak areas of peptides of corresponding protein expressed in the vehicle group)/mean of peak areas of the peptides of the corresponding protein expressed in the vehicle group. ↑ means increase, while ↓ means decrease. [e]Cannot be quantified by the method stated.

of this region was studied. Protein expressions in the somatosensory cortexes harvested from rats of the vehicle and MeHg groups fed for 12 weeks of MeHg were compared with ICPL labeling coupled LC-ESI-ion-trap MS/MS and LC-MALDI-TOF/TOF MS. Using the most commonly accepted criteria in proteomic studies for protein identification with high confidence, we positively identified 973 proteins in these somatosensory cortex samples (Figure 3A). After subjecting the data to a decoy database search, the maximum and minimum values of false positive identification rates for the LC-MALDI-TOF/TOF MS were estimated to be 0.87 and 0.11%, respectively. The maximum and minimum values of false identification using LC-ESI-ion-trap MS were estimated to be 0.94 and 0.34%, respectively. Consequently, proteins falsely identified were very low. Among the 973 proteins identified, 104 proteins were found to be differentially expressed in the somatosensory cortex of the rats after CELD intake of MeHg (Figure 3B). Detailed information of the differentially expressed proteins identified is presented in the Supporting Information, Table S2. Expression levels of these proteins were found to be either differentially increased by at least 32% or decreased by at least 22% of that of the vehicle group. Expression levels of 10 of these 104 proteins were selected for verification purposes using WB technologies. These 10 proteins were partially chosen because complementary antibodies were available commercially and partially because some of them hold pivotal positions for interactions of the various pathways. These pathways were visualized after bioinformatic analysis of the 104 differentially

dx.doi.org/10.1021/pr400356v | J. Proteome Res. 2013, 12, 5233−5245

expressed proteins. (See below.) WB of these 10 different proteins was performed on samples of the somatosensory cortexes collected from rats with CELD intake of MeHg. Expression levels of these 10 proteins agree with those obtained from the proteomic analysis (Table 2 and Figure S1 in the Supporting Information).

Bioinformatic pathway analysis of the 104 differentially expressed proteins using the KEGG database and PANTHER analysis placed these proteins into 10 categories (Figure 4).

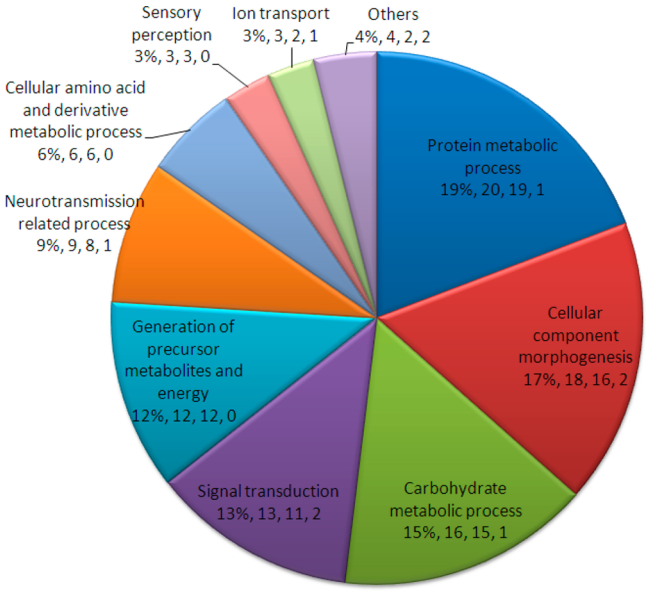

Figure 4. Pathway analysis of the differentially expressed proteins using gene orthology. Key to the labeling: In each label, the name of gene orthology category appears first, followed by percentage of protein (over the 104 proteins) clustered in this category, followed by the actual number of proteins clustered in this category, followed by the number of down-regulated proteins, followed by the number of protein up-regulated in this category.

Among these 10 categories, the "carbohydrate metabolic processes" as well as the "generation of precursor metabolites and energy" subgroups were directly related to ATP production. About 25% of the 104 differentially expressed proteins were involved. Another 20% of the differentially expressed proteins were involved in protein metabolism, including translation, protein complex assembly, and proteolysis. Moreover, other metabolic processes including those vital to maintain normal neuronal function were affected. These processes included the cellular component morphogenetic processes (17%), neurotransmission related process (9%), and the cellular amino acid as well as a derivative metabolic process (6%). These processes are responsible for maintaining the morphology of the neurons, neurite outgrowth, synaptic transmission, and production of glutamate, respectively. Furthermore, proteins related to the intracellular signal transduction (12%) and sensory perceptions (3%) were also affected. Clearly, our results implicate that the energy-generation processes and metabolic processes may be deficient in the somatosensory cortexes of rats loaded with submicromolar level of tHg by chronic exposure. Thus, selected verification experiments on the inhibitory effects of mercury accumulation of individual metabolic pathways were performed.

CELD of MeHg Altered the Levels of ATP, Pyruvate, and Ca in the S1 Area

Because of the apparent complexity of the interacting metabolic pathways, possible "cross-talking" among enzymes, and the presence of various feedback loops, three of the end products/participants of these metabolic pathways and neurotransmission processes were selected for verifications. The levels of ATP, pyruvate, and total calcium ions were measured in samples from the sham control, vehicle, and MeHg groups in the three sets of time points. First, ATP levels of the somatosensory cortexes harvested from the sham control and vehicle groups were around 40 to 45 nmol ATP per gram of tissue in the three time points (Figure 5A). For the MeHg group, ATP levels measured at the eighth week became lower than the controls. ATP levels of the samples from the 12th week MeHg group were significantly less than the rest of the samples ($p < 0.05$). Second, levels of pyruvate of the somatosensory cortexes harvested from the sham control and vehicle groups were around 10 to 15 nmol per gram of tissue (Figure 5B). Surprisingly, the pyruvate level in the MeHg group at fourth week was significantly higher than those in the sham control and vehicle groups ($p < 0.05$). Whether this result represented the onset of a transient compensatory mechanism is currently unknown. The pyruvate level in the MeHg group was reduced again in the 8th week sample, and the 12th week was significantly less than those in the sham control and vehicle groups ($p < 0.05$). Third, total calcium ion levels of the somatosensory cortexes harvested from the sham control and vehicle groups were around 7 to 8 ppm (micrograms Ca ions per gram of tissue) (Figure 5C). Conversely, Ca ion levels in the MeHg group at the fourth week were similar to those of the sham control and vehicle groups. On the 8th and 12th weeks, Ca ion levels in the MeHg group were significantly less than those of the other groups and at other time points ($p < 0.05$). Interestingly, only ~10% of the differentially expressed proteins in the MeHg group were up-regulated by >30% than the controls (Figure 1C). Details of their identities are shown in Table S4 of the Supporting Information. During pathway discovery, these up-regulated proteins were found to distribute sporadically and almost evenly among the 10 categories of down-regulated proteins (Figure 6). Because most of the proteins in each category were down-regulated, it is unlikely that these single/double up-regulated proteins would play a decisive role in reviving the metabolic deficit.

DISCUSSION

Mechanistic studies on MeHg intoxication have been performed for decades. However, most of these studies were performed with relatively large doses of MeHg done in an acute manner. Furthermore, cross-talking as well as interpathway effects in a global holistic manner have seldom been studied. This type of investigation was hampered by the lack of powerful proteomic analytical tools that we have today. Hence, only a handful of proteomic studies have been reported. One of the first studies was published in 2007, in which the effects of proteome changes of cerebellar granule cell culture after exposure to MeHg for 10 days were reported.[42] Resolved on 2-DE gels with silver staining, they could see around 800 protein spots. Several spots were identified by peptide-mass fingerprints. However, only one, mitochondrial 3-ketoacid-coenzyme A transferase I, was found to be decreased by 39% as compared with control cells treated with concentrations of MeHg (<300 nM Hg) that did not produce cytotoxic effects. The authors suggested that a failure of

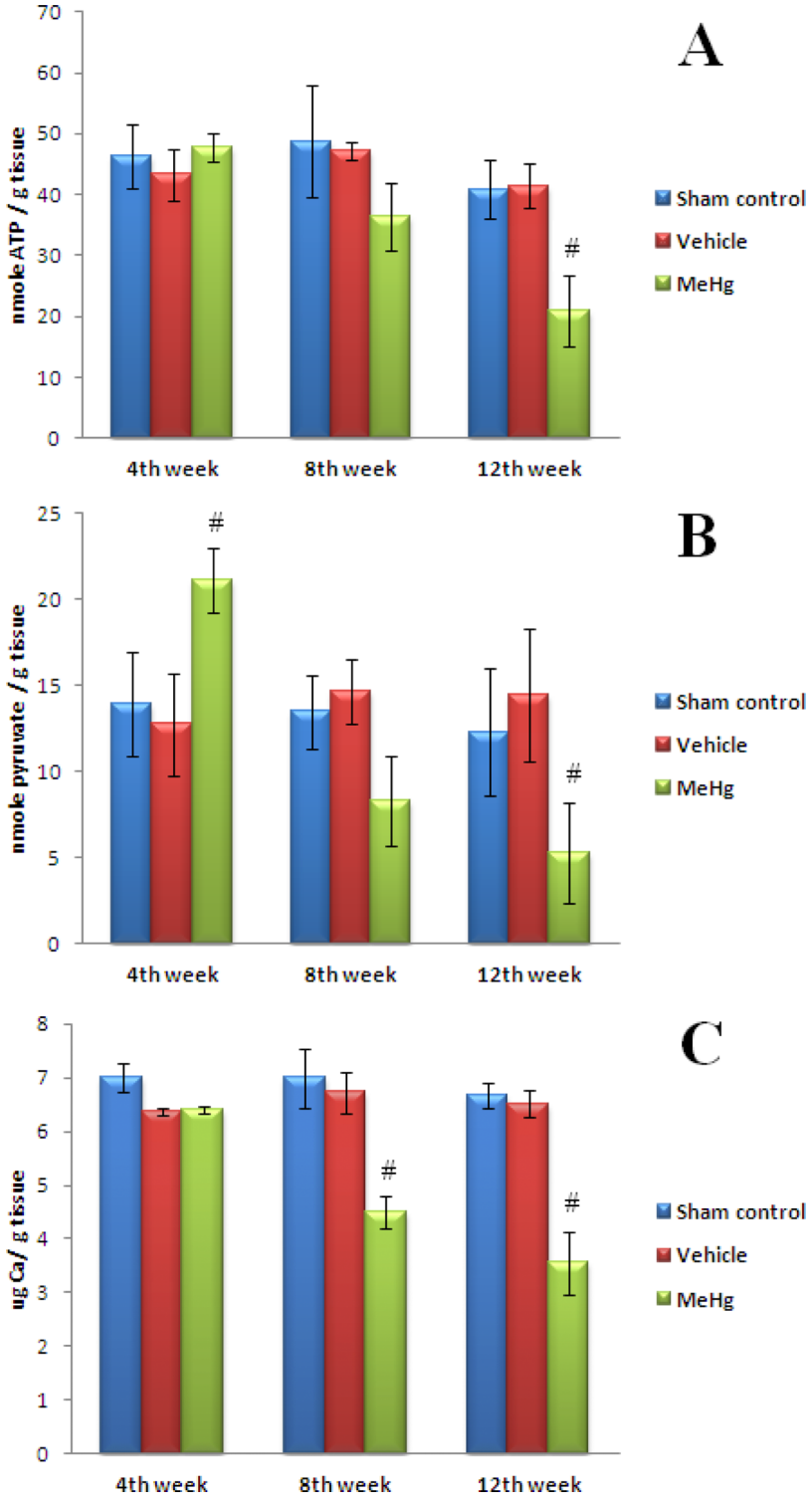

Figure 5. Levels of ATP, pyruvate, and Ca in the somatosensory cortexes harvested from different groups and at different time points. Each group at each time point contained 12 animals. (A) ATP levels. ATP levels in the MeHg group at 12th week were significantly less than the rest of the time points in the sham control, vehicle, and MeHg groups (#, $p < 0.05$). (B) Pyruvate levels. Pyruvate level in the MeHg group at 4th week was significantly higher than those in the sham control and vehicle groups (#, $p < 0.05$). The pyruvate levels in the MeHg group at 12th week were significantly lower than those in the sham control and vehicle groups (#, $p < 0.05$). (C) Calcium levels. Calcium levels in the MeHg group at the 8th and 12th week were significantly less than that in either the 4th week MeHg group or in the sham control and vehicle groups at any time points (#, $p < 0.05$).

mitochondrial metabolism might be an early event in the neurotoxicity induced by MeHg in the cerebellar granule cell culture. In 2009, after feeding juvenile beluga a diet containing 0.8 ppm MeHg for 70 days, Keyvanshokooh et al. found eight differentially expressed proteins in extracts of brain tissues from these animals.[43] These proteins were involved in cell metabolism, protein folding, cell division, and signal transduction. The authors suggested that MeHg exerts its toxicity through oxidative stress induction and apoptotic effects. They also suggested that chronic MeHg exposure could induce metabolic deficiency in the

dx.doi.org/10.1021/pr400356v | J. Proteome Res. 2013, 12, 5233−5245

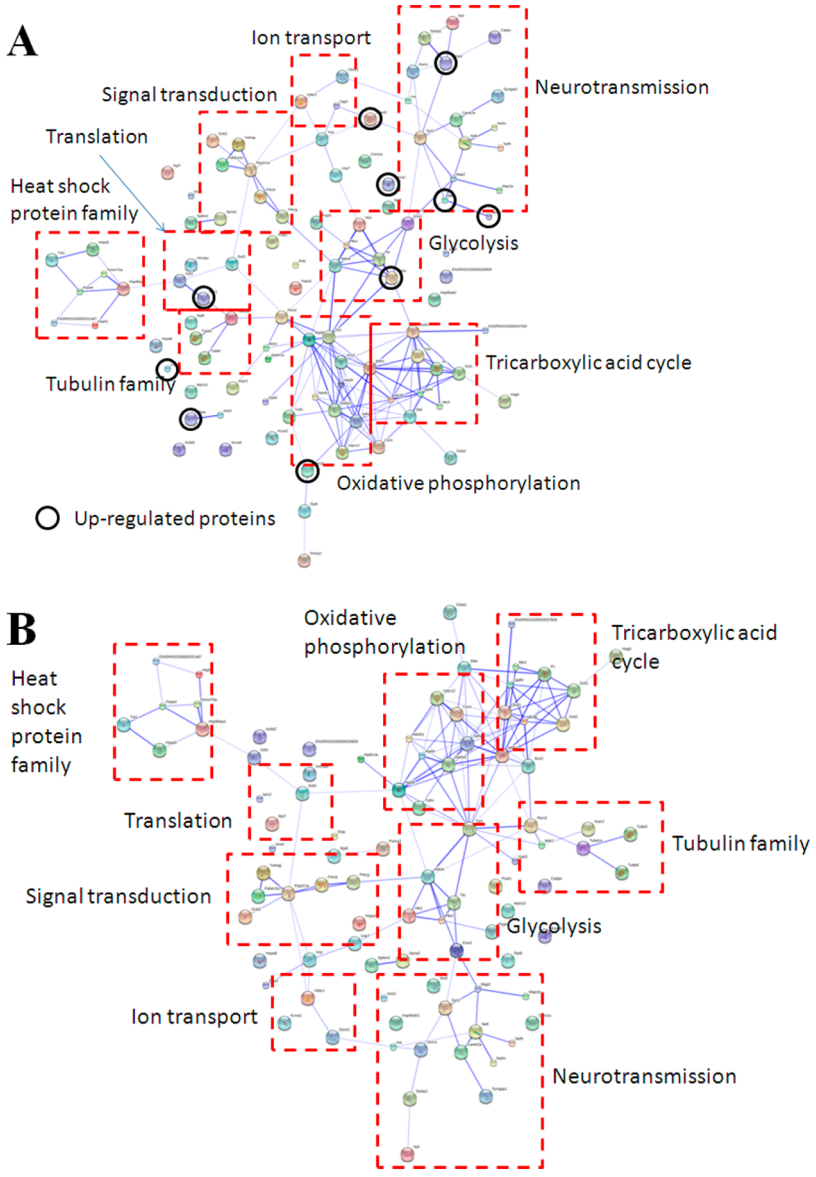

Figure 6. Confidence view of the protein−protein interaction (PPI) networks of the differentially expressed proteins as presented by STRING v9. Each spot represents one differentially expressed protein. The line joining two spots represents known interactions between these two proteins. More broad and intense lines indicate more evidence that was reported about the interactions between the proteins. Spots without any connection to the others means that there are no known interactions of these proteins within the 104 differentially expressed proteins in the STRING database. The PPI network was roughly divided into different areas (highlighted with red rectangles) based on their functional categories. (A) PPI network contained all of the differentially expressed proteins. Most of the differentially expressed proteins could be joined together, indicating the extent of cross-taking of these proteins and diversities of the different biological processes. The degree of inhibitory effects of accumulation of tHg in the somatosensory cortex was broad. Up-regulated proteins were circulated by black circles. It can be seen that none of them hold unique pivotal positions for interactions with the other pathways. (b) PPI network of down-regulated proteins alone. In the down-regulated PPI network, more intense interaction than that in panel A could be seen.

beluga brains.[43] Berg et al. (2010) injected Atlantic cod with either a total of 0.5 or 2 mg/kg MeHg intraperitoneally (first injection of half of the dose on the first day, with the remaining dose after 1 week). Using a combination of 2-DE, MALDI-TOF MS, and MS/MS, they observed the levels of 71 protein spots to be 20% or more significantly altered after MeHg exposure. Forty proteins were successfully identified, and they were known to be involved in mitochondrial dysfunction, oxidative stress, altered calcium homeostasis, and disruption of microtubules.[44] Results of our study are consistent with these studies. We found that many proteins involved in metabolism of carbohydrates, generation of precursor metabolites, and energy were down-regulated (Table S1 in the Supporting Information). Furthermore, in the 12 weeks CELD MeHg exposed rats, levels of ATP and pyruvate were found to be decreased in the somatosensory cortexes (Figure 5). These indicated that a metabolic deficit was induced in the somatosensory cortex after CELD of MeHg.

Apart from metabolic deficit, expressions of some proteins involved in the neural function were found to be up-regulated by more than two-fold (Table S4 in the Supporting Information). These included dihydropyrimidinase-like 2 protein (DPYSL-2), vesicle-associated membrane protein 2B, and myelin-associated oligodendrocyte basic protein. DPYSL-2 is responsible for neurite outgrowth.[45] It modulates axon outgrowth by direct

dx.doi.org/10.1021/pr400356v | J. Proteome Res. 2013, 12, 5233−5245

binding to tubulin and promotes the formation of microtubules.[46] Thus, it is believed that an up-regulation of DPYSL-2 in neurodegenerative diseases is a reactive response aimed to repair the damaged axons. Interestingly, DPYSL-2 was found to be up-regulated in Alzheimer's disease (AD).[47] It is speculated that MeHg may cause axon damages due to excitotoxicity, which in turn requires more DPYSL-2 for the repair process. Myelin-associated oligodendrocyte basic protein is also called myelin oligodendrocyte glycoprotein (MOG). Although the primary molecular function of MOG is not yet known, it is believed that it plays an important role in pathogenesis in demyelinating diseases of the central nervous system (CNS).[48] More specifically, MOG is speculated to be an adhesion molecule on the myelin sheath to provide its structural integrity.[49] It was known that progressive myelin degeneration was associated with MeHg accumulation in the CNS.[50] In addition, autopsy examination of CNS of a patient with Minamata disease found endoneurial fibrosis, regeneration of myelin sheaths, as well as loss of nerve fibers in dorsal roots and sural nerve.[51] Therefore, it is logical to implicate that the body needs overexpression of MOG to combat abnormalities in the myelin sheaths in somatosensory cortexes of rats with CELD of MeHg. Another overexpressed protein was vesicle-associated membrane protein 2B (VAMP-2). VAMP-2 is commonly found on the membrane surface of a vesicle and regulates endocytosis and exocytosis of the vesicle.[52] Gene expression of VAMP-2 was found to be up-regulated after neuronal injury in a rat model.[53] Thus, overexpression of VAMP-2 after CELD of MeHg may indicate that neuronal damage to the somatosensory cortex might occur. To summarize, it seems that up-regulations of these proteins could be countermeasures aimed to reverse some of the negative impact on the somatosensory cortex inflicted by CELD exposure of MeHg.

From another perspective, several epidemiological studies had implicated a positive correlation between MeHg exposure and prevalence of some neurodegenerative diseases. Lifelong exposure to MeHg was shown to be positively associated with the prevalence of PD in the Faroe Islands studies.[17] MeHg exposure may also increase the risk of having AD,[54,55] with the presence of dementia in an earlier age. As early as 2002, Weiss and coworkers predicted that chronic exposure of MeHg would result in erosion of neural cells numbers, followed by an compensatory increase in neurotransmitter output and development of additional synaptic connections.[56] This led to faster functional exhaustion than normal. The end result was that the neural cells underwent apoptosis earlier than they would normally.[56] In addition, recent studies on AD and PD discovered that the pathogenesis of these diseases shared some common characteristics, including lowered calcium buffering capacity and impaired mitochondrial function in the neurons.[57,58] In the current study, our proteomic data showed the down regulation of proteins that were involved in glycolysis, tricarboxylic acid cycle, respiratory electron transports chain, and Ca^{2+}-mediated signal transduction. The concomitant effects of accumulation of Hg in the somatosensory cortex were seen with decreased levels of pyruvate, ATP, and total Ca ions (Figure 5). Apparently, the current findings support that the metabolic deficit induced by CELD of MeHg shared some characteristics with the pathogenesis of some neurodegenerative diseases. Whether deficiency of these metabolically important compounds and decreased activities of many enzymes in the somatosensory cortex are confounding factors to the development of neurodegenerative diseases needs to be further studied. Nonetheless, the decreased activities of many metabolic important enzymes would certainly have negative impact on the normal functioning of neurons over time.

Lastly, the extent of the inhibitory effects of CELD of MeHg could be visualized by plotting the possible interactions of the differentially expressed proteins. PPIs of these 104 proteins were correlated and visualized with the STRING v.9 software. Interactive relationships of these differentially expressed proteins are shown by lines connecting them in Figure 6. The more broad and intense lines represent interactions that have higher confidence levels. It can be seen that there are more intense interactions in the clusters of the oxidative phosphorylation and translation, glycolysis, tricarboxylic acid cycle, neurotransmission, signal transduction, translation, ion transport, microtubules, as well as heat shock proteins. The extent of the inhibitory actions of CELD to MeHg in the somatosensory cortex is far and wide.

Overall, it is likely that the comparatively small amount of tHg accumulated in the brain inhibited many of the energy-generating metabolic pathways that resulted in a metabolic deficit state in the somatosensory cortex over time. Furthermore, interactions between many proteins/enzymes related to neurofilament production, microtubule production, myelin production, and neurotransmitter release were also affected. It is our working hypothesis that CELD to MeHg from the environment predisposes individuals to an energy-deficient state in the somatosensory cortex with reduction in the production of neurotransmitters as well as materials and energy that may be necessary for proper functioning and repair of the nervous system. Although results of this animal study cannot be extrapolated directly to humans, the effects of long-term low-dose intake of MeHg through consumption of fish present a serious concern. On one hand, with fish being a major source of protein intake in many populations, it is a necessary reality of everyday life. Many constituents in fish meat, including various kinds of polyunsaturated fatty acids, are beneficial to health, especially the circulatory system. On the other hand, it is also known that with the current level of use of fossil fuels and especially coal the level of MeHg in aquatic organisms will not decrease in the near future. The dilemma facing all public health administrators and educators regarding fish intake in the local context is difficult without the support of scientific information. This will not be an easy undertaking as more complex economic and aquacultural trade implications are also at play as well. Nonetheless, there is a pressing need to perform risk and benefit assessment studies regarding fish intake in fish-dependent as well as local populations in the local context.

■ CONCLUSIONS

To summarize, it seems likely that CELDs of MeHg induced a general state of metabolic deficit in the somatosensory cortex. A concomitant decrease in the levels of pyruvate, ATP, and total calcium ions was found. Such metabolic deficit may account for possible positive association between lifelong exposure to low doses of MeHg through seafood consumption and prevalence of neurodegenerative diseases.

■ ASSOCIATED CONTENT

Supporting Information

Minimum technical variabilities on relative protein quantification using ICPL labeling kit coupled with either ESI-ion-trap MS or MALDI-TOF/TOF MS; amount of total mercury (tHg) found in different parts of the rat brains harvested after feeding these rats with MeHg for 4, 8 and 12 weeks; results of Western blotting

dx.doi.org/10.1021/pr400356v | J. Proteome Res. 2013, 12, 5233−5245

validation of selected proteins of interest identified in the proteomic investigation part of this study; pathway analysis of the differentially expressed proteins using gene orthology; and identities of up-regulated proteins found in the somatosensory cortexes of 4 rats fed with 40 μg/kg body weight/day for 12 weeks. This material is available free of charge via the Internet at http://pubs.acs.org.

AUTHOR INFORMATION

Corresponding Author

*Tel: (852) 34008669. Fax: (852) 23649932. E-mail: samuel.chun-lap.lo@polyu.edu.hk.

Notes

The authors declare no competing financial interest.

ACKNOWLEDGMENTS

This work was supported by a Collaborative Research Fund from The Research Grant Council of Hong Kong awarded to M.-H.W. (account no.: HKBU1/07C, HK PolyU E-RD36) and by a grant from Research Committee of the Hong Kong Polytechnic University (G-YM34). H.-K.K. was supported by a Ph.D. studentship from HKBU1/07C. We acknowledge help from the technicians of the Shenzhen Research Institute of HKPU for the animal feeding work.

ABBREVIATIONS

ATP, adenosine triphosphate; CELD, chronic exposure to low doses; ESI-ion-trap MS/MS, electrospray ionization ion-trap tandem mass spectrometry; ICP-MS, inductively coupled plasma mass spectrometry; ICPL, isotope-coded protein labeling; JECFA, Joint FAO/WHO Expert Committee on Food Additives; LC, liquid chromatography; MALDI-TOF/TOF MS, matrix-assisted laser desorption ionization time-of-flight/time-of-flight mass spectrometry; MeHg, methylmercury; PUFAs, polyunsaturated fatty acids; PPI, protein−protein interaction; PTWI, provisional tolerable weekly intake; SDS-PAGE, sodium dodecyl sulfate polyacrylamide gel electrophoresis; S1 area, somatosensory area; Ca, total calcium; tHg, total mercury; WB, Western blot

REFERENCES

(1) Chen, C.; Amirbahman, A.; Fisher, N.; Harding, G.; Lamborg, C.; Nacci, D.; Taylor, D. Methylmercury in marine ecosystems: spatial patterns and processes of production, bioaccumulation, and biomagnification. *Ecohealth* **2008**, *5* (4), 399−408.

(2) Lam, H. S.; Kwok, K. M.; Chan, P. H.; So, H. K.; Li, A. M.; Ng, P. C.; Fok, T. F. Long term neurocognitive impact of low dose prenatal methylmercury exposure in Hong Kong. *Environ. Int.* **2013**, *54*, 59−64.

(3) Yorifuji, T.; Murata, K.; Bjerve, K. S.; Choi, A. L.; Weihe, P.; Grandjean, P. Visual evoked potentials in children prenatally exposed to methylmercury. *Neurotoxicology* **2013**, *37C*, 15−18.

(4) Murata, K.; Weihe, P.; Budtz-Jorgensen, E.; Jorgensen, P. J.; Grandjean, P. Correction for "Delayed brainstem auditory evoked potential latencies in 14-year-old children exposed to methylmercury" by Murata et al. *J. Pediatr.* **2006**, *149* (4), 583−584.

(5) Debes, F.; Budtz-Jorgensen, E.; Weihe, P.; White, R. F.; Grandjean, P. Impact of prenatal methylmercury exposure on neurobehavioral function at age 14 years. *Neurotoxicol. Teratol.* **2006**, *28* (5), 536−547.

(6) Castoldi, A. F.; Johansson, C.; Onishchenko, N.; Coccini, T.; Roda, E.; Vahter, M.; Ceccatelli, S.; Manzo, L. Human developmental neurotoxicity of methylmercury: impact of variables and risk modifiers. *Regul. Toxicol. Pharmacol.* **2008**, *51* (2), 201−214.

(7) Grandjean, P.; Satoh, H.; Murata, K.; Eto, K. Adverse effects of methylmercury: environmental health research implications. *Environ. Health Perspect.* **2010**, *118* (8), 1137−1145.

(8) Ortega-Garcia, J. A.; Rodriguez, K.; Calatayud, M.; Martin, M.; Velez, D.; Devesa, V.; Sanchez-Alarcon, M. C.; Torres Cantero, A. M.; Galindo-Cascales, C.; Gil-Vazquez, J. M.; Sanchez-Sauco, M. F.; Sanchez-Solis, M.; Alfonso-Marsilla, B.; Romero-Braquehais, F. Estimated intake levels of methylmercury in children, childbearing age and pregnant women in a Mediterranean region, Murcia, Spain. *Eur. J. Pediatr.* **2009**, *168* (9), 1075−1080.

(9) *Mercury in Fish and Food Safety*; Risk Assessment Studies Report No. 31; Centre for Food Safety, Food and Environmental Hygiene Department, The Government of the Hong Kong Special Administrative Region: Hong Kong, China, 2008.

(10) Phelps, R. W.; Clarkson, T. W.; Kershaw, T. G.; Wheatley, B. Interrelationships of blood and hair mercury concentrations in a North American population exposed to methylmercury. *Arch. Environ. Health* **1980**, *35* (3), 161−168.

(11) Budtz-Jorgensen, E.; Grandjean, P.; Keiding, N.; White, R. F.; Weihe, P. Benchmark dose calculations of methylmercury-associated neurobehavioural deficits. *Toxicol. Lett.* **2000**, *112*−*113*, 193−199.

(12) Johansen, P.; Mulvad, G.; Pedersen, H. S.; Hansen, J. C.; Riget, F. Human accumulation of mercury in Greenland. *Sci. Total Environ.* **2007**, *377* (2−3), 173−178.

(13) Cheng, J.; Gao, L.; Zhao, W.; Liu, X.; Sakamoto, M.; Wang, W. Mercury levels in fisherman and their household members in Zhoushan, China: impact of public health. *Sci. Total Environ.* **2009**, *407* (8), 2625−2630.

(14) Love, J. L.; Rush, G. M.; McGrath, H. Total mercury and methylmercury levels in some New Zealand commercial marine fish species. *Food Addit. Contam.* **2003**, *20* (1), 37−43.

(15) Stern, A. H.; Jacobson, J. L.; Ryan, L.; Burke, T. A. Do recent data from the Seychelles Islands alter the conclusions of the NRC Report on the toxicological effects of methylmercury? *Environ. Health* **2004**, *3* (1), 2.

(16) Al-Shahristani, H.; Al-Haddad, I. K. Mercury content of hair from normal and poisoned persons. *J. Radioanal. Nucl. Chem.* **1973**, *15* (1), 59−70.

(17) Petersen, M. S.; Halling, J.; Bech, S.; Wermuth, L.; Weihe, P.; Nielsen, F.; Jorgensen, P. J.; Budtz-Jorgensen, E.; Grandjean, P. Impact of dietary exposure to food contaminants on the risk of Parkinson's disease. *Neurotoxicology* **2008**, *29* (4), 584−590.

(18) Gump, B. B.; MacKenzie, J. A.; Dumas, A. K.; Palmer, C. D.; Parsons, P. J.; Segu, Z. M.; Mechref, Y. S.; Bendinskas, K. G. Fish consumption, low-level mercury, lipids, and inflammatory markers in children. *Environ. Res.* **2012**, *112*, 204−211.

(19) Takaoka, S.; Kawakami, Y.; Fujino, T.; Oh-ishi, F.; Motokura, F.; Kumagai, Y.; Miyaoka, T. Somatosensory disturbance by methylmercury exposure. *Environ. Res.* **2008**, *107* (1), 6−19.

(20) Yorifuji, T.; Tsuda, T.; Takao, S.; Suzuki, E.; Harada, M. Total mercury content in hair and neurologic signs: historic data from Minamata. *Epidemiology* **2009**, *20* (2), 188−193.

(21) Takaoka, S.; Fujino, T.; Sekikawa, T.; Miyaoka, T. Psychophysical sensory examination in individuals with a history of methylmercury exposure. *Environ. Res.* **2004**, *95* (2), 126−132.

(22) Edwards, J. R.; Marty, M. S.; Atchison, W. D. Comparative sensitivity of rat cerebellar neurons to dysregulation of divalent cation homeostasis and cytotoxicity caused by methylmercury. *Toxicol. Appl. Pharmacol.* **2005**, *208* (3), 222−232.

(23) Shapiro, A. M.; Chan, H. M. Characterization of demethylation of methylmercury in cultured astrocytes. *Chemosphere* **2008**, *74* (1), 112−118.

(24) Fonfria, E.; Vilaro, M. T.; Babot, Z.; Rodriguez-Farre, E.; Sunol, C. Mercury compounds disrupt neuronal glutamate transport in cultured mouse cerebellar granule cells. *J. Neurosci. Res.* **2005**, *79* (4), 545−553.

(25) Lawton, M.; Iqbal, M.; Kontovraki, M.; Lloyd Mills, C.; Hargreaves, A. J. Reduced tubulin tyrosination as an early marker of mercury toxicity in differentiating N2a cells. *Toxicol. In Vitro* **2007**, *21* (7), 1258−1261.

(26) Bornhausen, M.; Musch, H. R.; Greim, H. Operant behavior performance changes in rats after prenatal methylmercury exposure. *Toxicol. Appl. Pharmacol.* **1980**, *56* (3), 305−310.
(27) Buelke-Sam, J.; Kimmel, C. A.; Adams, J.; Nelson, C. J.; Vorhees, C. V.; Wright, D. C.; St Omer, V.; Korol, B. A.; Butcher, R. E.; Geyer, M. A.; et al. Collaborative Behavioral Teratology Study: results. *Neurobehav. Toxicol. Teratol.* **1985**, *7* (6), 591−624.
(28) (a) Eccles, C. U.; Annau, Z. Prenatal methyl mercury exposure: I. Alterations in neonatal activity. *Neurobehav. Toxicol. Teratol.* **1982**, *4* (3), 371−376. (b) Eccles, C. U.; Annau, Z. Prenatal methyl mercury exposure: II. Alterations in learning and psychotropic drug sensitivity in adult offspring. *Neurobehav. Toxicol. Teratol.* **1982**, *4* (3), 377−382.
(29) Vorhees, C. V. Behavioral effects of prenatal methylmercury in rats: a parallel trial to the Collaborative Behavioral Teratology Study. *Neurobehav. Toxicol. Teratol.* **1985**, *7* (6), 717−725.
(30) Fredriksson, A.; Gardlund, A. T.; Bergman, K.; Oskarsson, A.; Ohlin, B.; Danielsson, B.; Archer, T. Effects of maternal dietary supplementation with selenite on the postnatal development of rat offspring exposed to methyl mercury in utero. *Pharmacol. Toxicol.* **1993**, *72* (6), 377−382.
(31) Gao, Y.; Ding, Y.; Shi, R.; Tian, Y. Effects of methylmercury on postnatal neurobehavioral development in mice. *Neurotoxicol. Teratol.* **2008**, *30* (6), 462−467.
(32) Weiss, B.; Stern, S.; Cox, C.; Balys, M. Perinatal and lifetime exposure to methylmercury in the mouse: behavioral effects. *Neurotoxicology* **2005**, *26* (4), 675−690.
(33) Goulet, S.; Dore, F. Y.; Mirault, M. E. Neurobehavioral changes in mice chronically exposed to methylmercury during fetal and early postnatal development. *Neurotoxicol. Teratol.* **2003**, *25* (3), 335−347.
(34) Day, J. J.; Reed, M. N.; Newland, M. C. Neuromotor deficits and mercury concentrations in rats exposed to methyl mercury and fish oil. *Neurotoxicol. Teratol.* **2005**, *27* (4), 629−641.
(35) Charleston, J. S.; Bolender, R. P.; Mottet, N. K.; Body, R. L.; Vahter, M. E.; Burbacher, T. M. Increases in the number of reactive glia in the visual cortex of Macaca fascicularis following subclinical long-term methyl mercury exposure. *Toxicol. Appl. Pharmacol.* **1994**, *129* (2), 196−206.
(36) Rodrigues, J. L.; Serpeloni, J. M.; Batista, B. L.; Souza, S. S.; Barbosa, F., Jr. Identification and distribution of mercury species in rat tissues following administration of thimerosal or methylmercury. *Arch. Toxicol.* **2010**, *84* (11), 891−896.
(37) Schmidt, A.; Kellermann, J.; Lottspeich, F. A novel strategy for quantitative proteomics using isotope-coded protein labels. *Proteomics* **2005**, *5* (1), 4−15.
(38) Com, E.; Clavreul, A.; Lagarrigue, M.; Michalak, S.; Menei, P.; Pineau, C. Quantitative proteomic Isotope-Coded Protein Label (ICPL) analysis reveals alteration of several functional processes in the glioblastoma. *J. Proteomics* **2012**, *75* (13), 3898−3913.
(39) Papaioannou, M. D.; Lagarrigue, M.; Vejnar, C. E.; Rolland, A. D.; Kuhne, F.; Aubry, F.; Schaad, O.; Fort, A.; Descombes, P.; Neerman-Arbez, M.; Guillou, F.; Zdobnov, E. M.; Pineau, C.; Nef, S. Loss of Dicer in Sertoli cells has a major impact on the testicular proteome of mice. *Mol. Cell. Proteomics* **2010**, *10* (4), M900587−MCP200.
(40) Lee, C. H.; Lum, J. H.; Cheung, B. P.; Wong, M. S.; Butt, Y. K.; Tam, M. F.; Chan, W. Y.; Chow, C.; Hui, P. K.; Kwok, F. S.; Lo, S. C.; Fan, D. M. Identification of the heterogeneous nuclear ribonucleoprotein A2/B1 as the antigen for the gastrointestinal cancer specific monoclonal antibody MG7. *Proteomics* **2005**, *5* (4), 1160−1166.
(41) Khan, H. A. Bioluminometric assay of ATP in mouse brain: determinant factors for enhanced test sensitivity. *J. Biosci.* **2003**, *28* (4), 379−382.
(42) Vendrell, I.; Carrascal, M.; Vilaro, M. T.; Abian, J.; Rodriguez-Farre, E.; Sunol, C. Cell viability and proteomic analysis in cultured neurons exposed to methylmercury. *Hum. Exp. Toxicol.* **2007**, *26* (4), 263−272.
(43) Keyvanshokooh, S.; Vaziri, B.; Gharaei, A.; Mahboudi, F.; Esmaili-Sari, A.; Shahriari-Moghadam, M. Proteome modifications of juvenile beluga (Huso huso) brain as an effect of dietary methylmercury. *Comp. Biochem. Physiol., Part D: Genomics Proteomics* **2009**, *4* (4), 243−248.
(44) Berg, K.; Puntervoll, P.; Valdersnes, S.; Goksoyr, A. Responses in the brain proteome of Atlantic cod (Gadus morhua) exposed to methylmercury. *Aquat. Toxicol.* **2010**, *100* (1), 51−65.
(45) Quach, T. T.; Duchemin, A. M.; Rogemond, V.; Aguera, M.; Honnorat, J.; Belin, M. F.; Kolattukudy, P. E. Involvement of collapsin response mediator proteins in the neurite extension induced by neurotrophins in dorsal root ganglion neurons. *Mol. Cell. Neurosci.* **2004**, *25* (3), 433−443.
(46) Fukata, Y.; Itoh, T. J.; Kimura, T.; Menager, C.; Nishimura, T.; Shiromizu, T.; Watanabe, H.; Inagaki, N.; Iwamatsu, A.; Hotani, H.; Kaibuchi, K. CRMP-2 binds to tubulin heterodimers to promote microtubule assembly. *Nat. Cell Biol.* **2002**, *4* (8), 583−591.
(47) Castegna, A.; Aksenov, M.; Thongboonkerd, V.; Klein, J. B.; Pierce, W. M.; Booze, R.; Markesbery, W. R.; Butterfield, D. A. Proteomic identification of oxidatively modified proteins in Alzheimer's disease brain. Part II: dihydropyrimidinase-related protein 2, alpha-enolase and heat shock cognate 71. *J. Neurochem.* **2002**, *82* (6), 1524−1532.
(48) Reindl, M.; Di Pauli, F.; Rostasy, K.; Berger, T. The spectrum of MOG autoantibody-associated demyelinating diseases. *Nat. Rev. Neurol.* **2013**, *9*, 455−461.
(49) Wang, H.; Munger, K. L.; Reindl, M.; O'Reilly, E. J.; Levin, L. I.; Berger, T.; Ascherio, A. Myelin oligodendrocyte glycoprotein antibodies and multiple sclerosis in healthy young adults. *Neurology* **2008**, *71* (15), 1142−1146.
(50) Vinay, S. D.; Raghu, K. G.; Sood, P. P. Dose and duration related methylmercury deposition, glycosidases inhibition, myelin degeneration and chelation therapy. *Cell Mol. Biol.* **1990**, *36* (5), 609−623.
(51) Eto, K.; Tokunaga, H.; Nagashima, K.; Takeuchi, T. An autopsy case of minamata disease (methylmercury poisoning)−pathological viewpoints of peripheral nerves. *Toxicol. Pathol.* **2002**, *30* (6), 714−722.
(52) Burre, J.; Beckhaus, T.; Schagger, H.; Corvey, C.; Hofmann, S.; Karas, M.; Zimmermann, H.; Volknandt, W. Analysis of the synaptic vesicle proteome using three gel-based protein separation techniques. *Proteomics* **2006**, *6* (23), 6250−6262.
(53) Jacobsson, G.; Piehl, F.; Meister, B. VAMP-1 and VAMP-2 gene expression in rat spinal motoneurones: differential regulation after neuronal injury. *Eur. J. Neurosci.* **1998**, *10* (1), 301−316.
(54) Landrigan, P. J.; Sonawane, B.; Butler, R. N.; Trasande, L.; Callan, R.; Droller, D. Early environmental origins of neurodegenerative disease in later life. *Environ. Health Perspect.* **2005**, *113* (9), 1230−1233.
(55) Mutter, J.; Naumann, J.; Sadaghiani, C.; Schneider, R.; Walach, H. Alzheimer disease: mercury as pathogenetic factor and apolipoprotein E as a moderator. *Neuroendocrinol. Lett.* **2004**, *25* (5), 331−339.
(56) Weiss, B.; Clarkson, T. W.; Simon, W. Silent latency periods in methylmercury poisoning and in neurodegenerative disease. *Environ. Health Perspect.* **2002**, *110* (Suppl 5), 851−854.
(57) Du, H.; Guo, L.; Yan, S.; Sosunov, A. A.; McKhann, G. M.; Yan, S. S. Early deficits in synaptic mitochondria in an Alzheimer's disease mouse model. *Proc. Natl. Acad. Sci. U. S. A.* **2010**, *107* (43), 18670−18675.
(58) Jana, S.; Sinha, M.; Chanda, D.; Roy, T.; Banerjee, K.; Munshi, S.; Patro, B. S.; Chakrabarti, S. Mitochondrial dysfunction mediated by quinone oxidation products of dopamine: Implications in dopamine cytotoxicity and pathogenesis of Parkinson's disease. *Biochim. Biophys. Acta* **2011**, *1812* (6), 663−673.